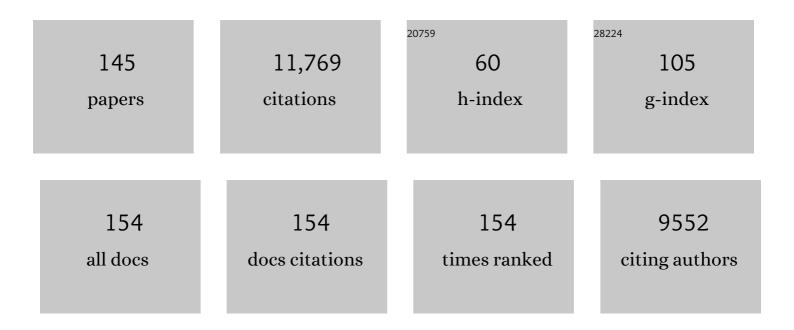
Xiaoli Tan

List of Publications by Year in descending order

Source: https://exaly.com/author-pdf/9301309/publications.pdf Version: 2024-02-01



Χιλοίι Τλη

#	Article	IF	CITATIONS
1	Removal of Pb(ii) ions from aqueous solutions on few-layered graphene oxide nanosheets. Dalton Transactions, 2011, 40, 10945.	1.6	488
2	Interaction between Eu(III) and Graphene Oxide Nanosheets Investigated by Batch and Extended X-ray Absorption Fine Structure Spectroscopy and by Modeling Techniques. Environmental Science & Technology, 2012, 46, 6020-6027.	4.6	470
3	Carbon-dot-supported atomically dispersed gold as a mitochondrial oxidative stress amplifier for cancer treatment. Nature Nanotechnology, 2019, 14, 379-387.	15.6	448
4	Removal of Pb(II) from aqueous solution by oxidized multiwalled carbon nanotubes. Journal of Hazardous Materials, 2008, 154, 407-416.	6.5	375
5	Eu(III) Sorption to TiO ₂ (Anatase and Rutile): Batch, XPS, and EXAFS Studies. Environmental Science & Technology, 2009, 43, 3115-3121.	4.6	347
6	One-Pot Synthesis of Water-Swellable Mg–Al Layered Double Hydroxides and Graphene Oxide Nanocomposites for Efficient Removal of As(V) from Aqueous Solutions. ACS Applied Materials & Interfaces, 2013, 5, 3304-3311.	4.0	310
7	Sorption of Eu(III) on Attapulgite Studied by Batch, XPS, and EXAFS Techniques. Environmental Science & Technology, 2009, 43, 5776-5782.	4.6	308
8	Sorption of Eu(III) on Humic Acid or Fulvic Acid Bound to Hydrous Alumina Studied by SEM-EDS, XPS, TRLFS, and Batch Techniques. Environmental Science & Technology, 2008, 42, 6532-6537.	4.6	272
9	Adsorption of Pb(II) from aqueous solution to MX-80 bentonite: Effect of pH, ionic strength, foreign ions and temperature. Applied Clay Science, 2008, 41, 37-46.	2.6	255
10	Cr(VI) Reduction and Immobilization by Core-Double-Shell Structured Magnetic Polydopamine@Zeolitic Idazolate Frameworks-8 Microspheres. ACS Sustainable Chemistry and Engineering, 2017, 5, 6795-6802.	3.2	211
11	Polyaniline-Modified Mg/Al Layered Double Hydroxide Composites and Their Application in Efficient Removal of Cr(VI). ACS Sustainable Chemistry and Engineering, 2016, 4, 4361-4369.	3.2	191
12	Comparative study of graphene oxide, activated carbon and carbon nanotubes as adsorbents for copper decontamination. Dalton Transactions, 2013, 42, 5266.	1.6	188
13	Adsorption kinetic, thermodynamic and desorption studies of Th(IV) on oxidized multi-wall carbon nanotubes. Colloids and Surfaces A: Physicochemical and Engineering Aspects, 2007, 302, 449-454.	2.3	186
14	Counterion effects of nickel and sodium dodecylbenzene sulfonate adsorption to multiwalled carbon nanotubes in aqueous solution. Carbon, 2008, 46, 1741-1750.	5.4	186
15	Polyaniline-modified 3D-flower-like molybdenum disulfide composite for efficient adsorption/photocatalytic reduction of Cr(VI). Journal of Colloid and Interface Science, 2016, 476, 62-70.	5.0	185
16	Experimental and theoretical studies on competitive adsorption of aromatic compounds on reduced graphene oxides. Journal of Materials Chemistry A, 2016, 4, 5654-5662.	5.2	185
17	Adsorption of Eu(III) onto TiO2: Effect of pH, concentration, ionic strength and soil fulvic acid. Journal of Hazardous Materials, 2009, 168, 458-465.	6.5	183
18	Macroscopic and Microscopic Investigation of Ni(II) Sequestration on Diatomite by Batch, XPS, and EXAFS Techniques. Environmental Science & Technology, 2011, 45, 7718-7726.	4.6	172

#	Article	IF	CITATIONS
19	Highly efficient removal of U(VI) by the photoreduction of SnO2/CdCO3/CdS nanocomposite under visible light irradiation. Applied Catalysis B: Environmental, 2020, 279, 119390.	10.8	166
20	Surface complexation modeling of Sr(II) and Eu(III) adsorption onto oxidized multiwall carbon nanotubes. Journal of Colloid and Interface Science, 2008, 323, 33-41.	5.0	163
21	Sorption of radionuclides from aqueous systems onto graphene oxide-based materials: a review. Inorganic Chemistry Frontiers, 2015, 2, 593-612.	3.0	154
22	Effect of surfactants on Pb(II) adsorption from aqueous solutions using oxidized multiwall carbon nanotubes. Chemical Engineering Journal, 2011, 166, 551-558.	6.6	151
23	Coexistence of adsorption and coagulation processes of both arsenate and NOM from contaminated groundwater by nanocrystallined Mg/Al layered double hydroxides. Water Research, 2013, 47, 4159-4168.	5.3	150
24	A core–shell structure of polyaniline coated protonic titanate nanobelt composites for both Cr(<scp>vi</scp>) and humic acid removal. Polymer Chemistry, 2016, 7, 785-794.	1.9	146
25	Comparison of U(VI) removal from contaminated groundwater by nanoporous alumina and non-nanoporous alumina. Separation and Purification Technology, 2011, 83, 196-203.	3.9	144
26	Impact of Al ₂ O ₃ on the Aggregation and Deposition of Graphene Oxide. Environmental Science & Technology, 2014, 48, 5493-5500.	4.6	144
27	Sorption Speciation of Lanthanides/Actinides on Minerals by TRLFS, EXAFS and DFT Studies: A Review. Molecules, 2010, 15, 8431-8468.	1.7	143
28	In situ carbothermal reduction synthesis of Fe nanocrystals embedded into N-doped carbon nanospheres for highly efficient U(VI) adsorption and reduction. Chemical Engineering Journal, 2018, 331, 395-405.	6.6	140
29	Water-soluble polyacrylamide coated-Fe3O4 magnetic composites for high-efficient enrichment of U(VI) from radioactive wastewater. Chemical Engineering Journal, 2014, 246, 268-276.	6.6	137
30	Sorption and desorption of Th(IV) on nanoparticles of anatase studied by batch and spectroscopy methods. Colloids and Surfaces A: Physicochemical and Engineering Aspects, 2007, 296, 109-116.	2.3	135
31	Sorption of Ni2+ on Na-rectorite studied by batch and spectroscopy methods. Applied Geochemistry, 2008, 23, 2767-2777.	1.4	119
32	Effect of soil humic and fulvic acids, pH and ionic strength on Th(IV) sorption to TiO2 nanoparticles. Applied Radiation and Isotopes, 2007, 65, 375-381.	0.7	117
33	Efficient removal of Pb ²⁺ by Tb-MOFs: identifying the adsorption mechanism through experimental and theoretical investigations. Environmental Science: Nano, 2019, 6, 261-272.	2.2	111
34	Effect of pH and Aging Time on the Kinetic Dissociation of243Am(III) from Humic Acid-Coated γ-Al2O3: A Chelating Resin Exchange Study. Environmental Science & Technology, 2005, 39, 7084-7088.	4.6	109
35	Magnetic Porous Polymers Prepared via High Internal Phase Emulsions for Efficient Removal of Pb ²⁺ and Cd ²⁺ . ACS Sustainable Chemistry and Engineering, 2018, 6, 5206-5213.	3.2	106
36	Recent Progress on Metal-Enhanced Photocatalysis: A Review on the Mechanism. Research, 2021, 2021, 9794329.	2.8	101

#	Article	IF	CITATIONS
37	Influence of soil humic acid and fulvic acid on sorption of thorium(IV) on MX-80 bentonite. Radiochimica Acta, 2006, 94, 429-434.	0.5	95
38	Sorption of Pb(II) on Na-rectorite: Effects of pH, ionic strength, temperature, soil humic acid and fulvic acid. Colloids and Surfaces A: Physicochemical and Engineering Aspects, 2008, 328, 8-14.	2.3	95
39	Effect of pH, ionic strength and temperature on sorption of Pb(II) on NKF-6 zeolite studied by batch technique. Chemical Engineering Journal, 2011, 168, 86-93.	6.6	91
40	Porous biochar modified with polyethyleneimine (PEI) for effective enrichment of U(VI) in aqueous solution. Science of the Total Environment, 2020, 708, 134575.	3.9	89
41	New Insight into GO, Cadmium(II), Phosphate Interaction and Its Role in GO Colloidal Behavior. Environmental Science & Technology, 2016, 50, 9361-9369.	4.6	85
42	Biochar Derived from Sawdust Embedded with Molybdenum Disulfide for Highly Selective Removal of Pb ²⁺ . ACS Applied Nano Materials, 2018, 1, 2689-2698.	2.4	85
43	Low-temperature synthesis of Mn3O4 hollow-tetrakaidecahedrons and their application in electrochemical capacitors. CrystEngComm, 2011, 13, 4915.	1.3	84
44	Impact of graphene oxide on the antibacterial activity of antibiotics against bacteria. Environmental Science: Nano, 2017, 4, 1016-1024.	2.2	84
45	Coupling g-C3N4 nanosheets with metal-organic frameworks as 2D/3D composite for the synergetic removal of uranyl ions from aqueous solution. Journal of Colloid and Interface Science, 2019, 550, 117-127.	5.0	84
46	Rapid and selective uranium extraction from aqueous solution under visible light in the absence of solid photocatalyst. Science China Chemistry, 2021, 64, 1323-1331.	4.2	75
47	Diffusion and sorption of U(VI) in compacted bentonite studied by a capillary method. Radiochimica Acta, 2005, 93, 273-278.	0.5	73
48	Sorption of Th(IV) on Na-rectorite: Effect of HA, ionic strength, foreign ions and temperature. Applied Geochemistry, 2007, 22, 2892-2906.	1.4	72
49	Adsorption and kinetic desorption study of ¹⁵²⁺¹⁵⁴ Eu(III) on multiwall carbon nanotubes from aqueous solution by using chelating resin and XPS methods. Radiochimica Acta, 2008, 96, 23-29.	0.5	72
50	Highly efficient uranium extraction by a piezo catalytic reduction-oxidation process. Applied Catalysis B: Environmental, 2022, 310, 121343.	10.8	72
51	Interaction Mechanism of Re(VII) with Zirconium Dioxide Nanoparticles Archored onto Reduced Graphene Oxides. ACS Sustainable Chemistry and Engineering, 2017, 5, 2163-2171.	3.2	70
52	Effect of Silicate on the Formation and Stability of Ni–Al LDH at the γ-Al ₂ O ₃ Surface. Environmental Science & Technology, 2014, 48, 13138-13145.	4.6	68
53	Analytical approaches to the speciation of lanthanides at solid-water interfaces. TrAC - Trends in Analytical Chemistry, 2014, 61, 107-132.	5.8	66
54	Core–shell hierarchical C@Na ₂ Ti ₃ O ₇ ·9H ₂ O nanostructures for the efficient removal of radionuclides. Environmental Science: Nano, 2018, 5, 1140-1149.	2.2	66

#	Article	IF	CITATIONS
55	Comparative study of Pb(II) sorption on XC-72 carbon and multi-walled carbon nanotubes from aqueous solutions. Chemical Engineering Journal, 2011, 170, 170-177.	6.6	65
56	Two-dimensional copper-based metalâ~'organic frameworks nano-sheets composites: One-step synthesis and highly efficient U(VI) immobilization. Journal of Hazardous Materials, 2019, 373, 580-590.	6.5	65
57	Insights into key factors controlling GO stability in natural surface waters. Journal of Hazardous Materials, 2017, 335, 56-65.	6.5	64
58	Phosphate functionalized layered double hydroxides (phos-LDH) for ultrafast and efficient U(VI) uptake from polluted solutions. Journal of Hazardous Materials, 2020, 399, 123081.	6.5	64
59	Spectroscopic and modeling investigation of efficient removal of U(VI) on a novel magnesium silicate/diatomite. Separation and Purification Technology, 2017, 174, 425-431.	3.9	63
60	Systematic studies on the binding of metal ions in aggregates of humic acid: Aggregation kinetics, spectroscopic analyses and MD simulations. Environmental Pollution, 2019, 246, 999-1007.	3.7	62
61	Effect of silicate on U(VI) sorption to γ-Al2O3: Batch and EXAFS studies. Chemical Engineering Journal, 2015, 269, 371-378.	6.6	60
62	Fabrication of hierarchical core-shell polydopamine@MgAl-LDHs composites for the efficient enrichment of radionuclides. Applied Surface Science, 2017, 396, 1726-1735.	3.1	60
63	Fabrication of Core–Shell CMNP@PmPD Nanocomposite for Efficient As(V) Adsorption and Reduction. ACS Sustainable Chemistry and Engineering, 2017, 5, 4399-4407.	3.2	57
64	Metal-organic frameworks-derived 3D yolk shell-like structure Ni@carbon as a recyclable catalyst for Cr(VI) reduction. Chemical Engineering Journal, 2020, 389, 123428.	6.6	57
65	Sorption Speciation of Nickel(ii) onto Ca-Montmorillonite: Batch, EXAFS Techniques and Modeling. Dalton Transactions, 2011, 40, 10953.	1.6	54
66	Mutual effects of copper and phosphate on their interaction with γ-Al2O3: Combined batch macroscopic experiments with DFT calculations. Journal of Hazardous Materials, 2012, 237-238, 199-208.	6.5	53
67	Impact of environmental conditions on the sorption behavior of radionuclide 90 Sr(II) on Na-montmorillonite. Journal of Molecular Liquids, 2015, 203, 39-46.	2.3	53
68	Sorption and complexation of Eu(III) on alumina: Effects of pH, ionic strength, humic acid and chelating resin on kinetic dissociation study. Applied Radiation and Isotopes, 2006, 64, 414-421.	0.7	52
69	Multifunctional flexible free-standing titanate nanobelt membranes as efficient sorbents for the removal of radioactive 90Sr2+ and 137Cs+ ions and oils. Scientific Reports, 2016, 6, 20920.	1.6	52
70	Core-shell CMNP@PDAP nanocomposites for simultaneous removal of chromium and arsenic. Chemical Engineering Journal, 2018, 349, 481-490.	6.6	52
71	Characterization of Lin'an montmorillonite and its application in the removal of Ni ²⁺ from aqueous solutions. Radiochimica Acta, 2008, 96, 487-495.	0.5	51
72	Bonding properties of humic acid with attapulgite and its influence on U(VI) sorption. Chemical Geology, 2017, 464, 91-100.	1.4	51

#	Article	IF	CITATIONS
73	Synthesis of a core–shell magnetic Fe ₃ O ₄ –NH ₂ @PmPD nanocomposite for efficient removal of Cr(<scp>vi</scp>) from aqueous media. RSC Advances, 2017, 7, 36231-36241.	1.7	51
74	Fully phosphorylated 3D graphene oxide foam for the significantly enhanced U(VI) sequestration. Environmental Pollution, 2019, 249, 434-442.	3.7	50
75	Insight into the performance and mechanism of low-cost phytic acid modified Zn-Al-Ti LMO for U(VI) removal. Chemical Engineering Journal, 2020, 402, 125510.	6.6	50
76	Sorption behavior of Co(II) on γ-Al2O3 in the presence of humic acid. Journal of Radioanalytical and Nuclear Chemistry, 2007, 273, 227-233.	0.7	48
77	Investigation of radionuclide 63Ni(II) sequestration mechanisms on mordenite by batch and EXAFS spectroscopy study. Science China Chemistry, 2012, 55, 632-642.	4.2	48
78	Symmetry-breaking induced piezocatalysis of Bi2S3 nanorods and boosted by alternating magnetic field. Applied Catalysis B: Environmental, 2022, 316, 121664.	10.8	48
79	SnO2 hierarchical nanostructure and its strong narrow-band photoluminescence. Journal of Materials Chemistry, 2009, 19, 1320.	6.7	45
80	Eu(III) uptake on rectorite in the presence of humic acid: A macroscopic and spectroscopic study. Journal of Colloid and Interface Science, 2013, 393, 249-256.	5.0	45
81	Coagulation behavior of humic acid in aqueous solutions containing Cs+, Sr2+ and Eu3+: DLS, EEM and MD simulations. Environmental Pollution, 2018, 236, 835-843.	3.7	41
82	Selective Immobilization of Highly Valent Radionuclides by Carboxyl Functionalized Mesoporous Silica Microspheres: Batch, XPS, and EXAFS Analyses. ACS Sustainable Chemistry and Engineering, 2018, 6, 15644-15652.	3.2	41
83	Effect of humic acid on nickel(ii) sorption to Ca-montmorillonite by batch and EXAFS techniques study. Dalton Transactions, 2012, 41, 10803.	1.6	39
84	Theoretical investigation of uranyl ion adsorption on hydroxylated Î ³ -Al2O3 surfaces. RSC Advances, 2013, 3, 19551.	1.7	37
85	Interaction mechanism of radionickel on Na-montmorillonite: Influences of pH, electrolyte cations, humic acid and temperature. Chemical Engineering Journal, 2016, 302, 77-85.	6.6	37
86	K2Ti6O13 hybridized graphene oxide: Effective enhancement in photodegradation of RhB and photoreduction of U(VI). Environmental Pollution, 2019, 248, 448-455.	3.7	37
87	The concentration and pH dependent diffusion of 137Cs in compacted bentonite by using capillary method. Journal of Nuclear Materials, 2005, 345, 184-191.	1.3	32
88	Design of Chitosan-Grafted Carbon Nanotubes: Evaluation of How the –OH Functional Group Affects Cs+ Adsorption. Marine Drugs, 2015, 13, 3116-3131.	2.2	32
89	Mutual effects behind the simultaneous U(VI) and humic acid adsorption by hierarchical MWCNT/ZIF-8 composites. Journal of Molecular Liquids, 2019, 288, 110971.	2.3	31
90	Enhancement of Rb+ and Cs+ removal in 3D carbon aerogel-supported Na2Ti3O7. Journal of Molecular Liquids, 2018, 262, 476-483.	2.3	30

#	Article	IF	CITATIONS
91	Preparation of TiO ₂ /Multiwalled Carbon Nanotube Composites and Their Applications in Photocatalytic Reduction of Cr(VI) Study. Journal of Nanoscience and Nanotechnology, 2008, 8, 5624-5631.	0.9	29
92	Fabrication and Photoluminescence Property of SnO ₂ Microtowers with Interstitial Tin Ions. Journal of Physical Chemistry C, 2009, 113, 9676-9680.	1.5	29
93	Efficient capture of ReO4â^' on magnetic amine-functionalized MIL-101(Cr): Revealing from selectivity to mechanism. Science of the Total Environment, 2021, 771, 144840.	3.9	29
94	Sorption and desorption of Eu(III) on alumina. Journal of Radioanalytical and Nuclear Chemistry, 2005, 266, 419-424.	0.7	28
95	Microscopic level investigation of Ni(II) sorption on Na-rectorite by EXAFS technique combined with statistical F-tests. Journal of Hazardous Materials, 2013, 252-253, 2-10.	6.5	28
96	Controlled synthesized natroalunite microtubes applied for cadmium(II) and phosphate co–removal. Journal of Hazardous Materials, 2016, 314, 249-259.	6.5	26
97	The synergetic enhancement of piezo catalytic performance to remove tetracycline by K2Ti6O13/TiO2 composite. Journal of Alloys and Compounds, 2022, 900, 163492.	2.8	25
98	Effect of pH, humic acid and addition sequences on Eu(III) sorption onto γ-Al2O3 study by batch and time resolved laser fluorescence spectroscopy. Chemical Engineering Journal, 2016, 287, 313-320.	6.6	24
99	Study of nano-Au-assembled amperometric CO gas sensor. Sensors and Actuators B: Chemical, 2005, 107, 866-871.	4.0	23
100	Critical Evaluation of Adsorption–Desorption Hysteresis of Heavy Metal Ions from Carbon Nanotubes: Influence of Wall Number and Surface Functionalization. Chemistry - an Asian Journal, 2014, 9, 1144-1151.	1.7	23
101	U(VI) adsorption on hematite nanocrystals: Insights into the reactivity of {001} and {012} facets. Journal of Hazardous Materials, 2020, 399, 123028.	6.5	23
102	Co-sequestration of Zn(II) and phosphate by γ-Al2O3: From macroscopic to microscopic investigation. Journal of Hazardous Materials, 2015, 297, 134-145.	6.5	22
103	The influence of dissolved Si on Ni precipitate formation at the kaolinite water interface: Kinetics, DRS and EXAFS analysis. Chemosphere, 2017, 173, 135-142.	4.2	21
104	Fabrication of core–shell α-MnO ₂ @polydopamine nanocomposites for the efficient and ultra-fast removal of U(<scp>vi</scp>) from aqueous solution. Dalton Transactions, 2019, 48, 971-981.	1.6	21
105	Retention of U(VI) by the Formation of Fe Precipitates from Oxidation of Fe(II). ACS Earth and Space Chemistry, 2018, 2, 968-976.	1.2	20
106	One-dimensional hollow SrS nanostructure with red long-lasting phosphorescence. Journal of Alloys and Compounds, 2008, 457, 413-416.	2.8	19
107	Simulation of radionuclides 99Tc and 243Am migration in compacted bentonite. Applied Radiation and Isotopes, 2005, 62, 759-764.	0.7	18
108	Hydrothermal deposition of titanate on biomass carbonaceous aerogel to prepare novel biomass adsorbents for Rb+ and Cs+. Colloids and Surfaces A: Physicochemical and Engineering Aspects, 2020, 590, 124501.	2.3	18

#	Article	IF	CITATIONS
109	Impurity induced formation of Sn2+ions in SnO2and the photoluminescence property. Journal Physics D: Applied Physics, 2007, 40, 7648-7651.	1.3	17
110	Investigation of radionuclide 60Co(II) binding to TiO2 by batch technique, surface complexation model and DFT calculations. Science China Chemistry, 2012, 55, 1752-1759.	4.2	17
111	Improvement of U(VI) removal by tuning magnetic metal organic frameworks with amine ligands. Journal of Molecular Liquids, 2021, 334, 116495.	2.3	17
112	A green and economical MgO/biochar composite for the removal of U(VI) from aqueous solutions. Chemical Engineering Research and Design, 2022, 180, 391-401.	2.7	17
113	Ammonium molybdophosphate/metal-organic framework composite as an effective adsorbent for capture of Rb+ and Cs+ from aqueous solution. Journal of Solid State Chemistry, 2022, 306, 122767.	1.4	16
114	Investigation of U(VI) sorption on silica aerogels: Effects of specific surface area, pH and coexistent electrolyte ions. Journal of Molecular Liquids, 2017, 246, 140-148.	2.3	15
115	Plasma-facilitated modification of pumpkin vine-based biochar and its application for efficient elimination of uranyl from aqueous solution. Plasma Science and Technology, 2019, 21, 095502.	0.7	15
116	Retention of Pb(II) by a Low-Cost Magnetic Composite Prepared by Environmentally-Friendly Plasma Technique. Separation Science and Technology, 2013, 48, 1211-1219.	1.3	14
117	Influence of pH, soil humic acid, ionic strength and temperature on sorption of U(VI) onto attapulgite. Journal of Radioanalytical and Nuclear Chemistry, 2018, 316, 981-991.	0.7	13
118	Designed Core–Shell Fe3O4@Polydopamine for Effectively Removing Uranium(VI) from Aqueous Solution. Bulletin of Environmental Contamination and Toxicology, 2021, 106, 165-174.	1.3	13
119	A carboxymethyl cellulose modified magnetic bentonite composite for efficient enrichment of radionuclides. RSC Advances, 2016, 6, 65136-65145.	1.7	12
120	Characterization of Fe(III)-saturated montmorillonite and evaluation its sorption behavior for U(VI). Radiochimica Acta, 2016, 104, 481-490.	0.5	12
121	Effect of co-existing Co2+ ions on the aggregation of humic acid in aquatic environment: Aggregation kinetics, dynamic properties and fluorescence spectroscopic study. Science of the Total Environment, 2019, 674, 544-553.	3.9	12
122	Novel Biomassâ€Derived Adsorbents Grafted Sodium Titanium Silicate with High Adsorption Capacity for Rb + and Cs + in the Brine. ChemistrySelect, 2019, 4, 13630-13637.	0.7	12
123	Nanoscale Pt ₅ Ni ₃₆ design and synthesis for efficient oxygen reduction reaction in proton exchange membrane fuel cells. Journal of Materials Chemistry A, 2021, 9, 21051-21056.	5.2	12
124	Super-efficient extraction of U(VI) by the dual-functional sodium vanadate (Na2V6O16·2H2O) nanobelts. Chemical Engineering Journal, 2022, 446, 137230.	6.6	12
125	Synthesis and study of the surface properties of long-chain alkylnaphthalene sulfonates. Journal of Surfactants and Detergents, 2004, 7, 135-139.	1.0	11
126	XPS investigation of impurities containing boron films affected by energetic deuterium implantation and thermal desorption. Journal of Nuclear Materials, 2015, 457, 118-123.	1.3	11

#	Article	IF	CITATIONS
127	Template-free fabrication of SnO2 hollow spheres with photoluminescence from Sni. Materials Letters, 2010, 64, 2033-2035.	1.3	10
128	High density near amorphous InSb nanowire arrays and its photo-electric performance. Journal of Alloys and Compounds, 2015, 626, 35-41.	2.8	10
129	FeOOH nanorods array and its application in the photoreduction of Cr(VI). Materials Letters, 2018, 231, 76-79.	1.3	10
130	Stress modulation on photodegradation of tetracycline by Sn-doped BiOBr. Journal of Environmental Chemical Engineering, 2022, 10, 107675.	3.3	10
131	Effects of humic acid and Mg2+ on morphology and aggregation behavior of silica aerogels. Journal of Molecular Liquids, 2018, 264, 261-268.	2.3	9
132	Homogeneous Ni nanoparticles anchored on mesoporous N-doped carbon as highly efficient catalysts for Cr(VI), tetracycline and dyes reduction. Applied Surface Science, 2022, 575, 151748.	3.1	9
133	Insights into mechanism on organic acids assisted translocation of uranium in Brassica juncea var. foliosa by EXAFS. Journal of Environmental Radioactivity, 2020, 218, 106254.	0.9	8
134	State-of-the-art progress for the selective crystallization of actinides, synthesis of actinide compounds and their functionalization. Journal of Hazardous Materials, 2022, 426, 127838.	6.5	8
135	Selective and efficient removal of radioactive ions from water with well-dispersed metal oxide nanoparticles@N-doped carbon. Separation and Purification Technology, 2022, 285, 120366.	3.9	8
136	Effect of silicate on the sorption properties of kaolinite: removal of U(VI) and mechanism. Journal of Radioanalytical and Nuclear Chemistry, 2017, 311, 1899-1907.	0.7	6
137	The investigation on the mechanism of the increased decay time in red SrS:Eu2+,Dy3+ phosphor. Materials Chemistry and Physics, 2018, 207, 161-166.	2.0	4
138	Enhanced catalytic reduction of Cr(VI) with formic acid over spherical bimetallic Ni-Co nanoalloy catalysts at room temperature. Applied Surface Science, 2022, 601, 154252.	3.1	4
139	Evaluation of the influence of environmental conditions on the removal of Pb(II) from wastewater by Ca-rectorite. Separation Science and Technology, 2015, , 150623132817002.	1.3	3
140	Kinetic and thermodynamic studies on the interaction of europium(III) and phosphate with γ-Al2O3. Journal of Radioanalytical and Nuclear Chemistry, 2017, 311, 395-408.	0.7	3
141	Au@SiO2 hybridized Ca2B2O5·H2O:Tb3+ nano belts: An insight on the enhanced photoluminescence by Au nanoparticles. Journal of Alloys and Compounds, 2019, 784, 354-361.	2.8	3
142	Construction of Ni-based N-doped mesoporous carbon sphere for efficiently catalytic dichromate reduction with HCOOH at room temperature. Separation and Purification Technology, 2022, 295, 121289.	3.9	3
143	Characterization of the sorption behavior and mechanism of U(VI) on sericite by batch experiments and spectroscopic techniques. Journal of Radioanalytical and Nuclear Chemistry, 2017, 313, 333-342.	0.7	1
144	Interactions between radionuclides and the oxide-water interfaces in the environment. Interface Science and Technology, 2019, 29, 39-105.	1.6	1

#	Article	IF	CITATIONS
145	Water treatment and environmental remediation applications of carbon-based nanomaterials. , 2022, , 229-311.		0